# Growth of Polystyrene Domains in Isotropic, Nematic and Smectic Phase of 8CB Liquid Crystal

**M. Graca,[†] S. A. Wieczorek,[†,*] and R. Hołyst[†,‡]**

*Institute of Physical Chemistry PAS, Department III, Kasprzaka 44/52, 01-224 Warsaw, Poland, and WMP-SNS, Cardinal Stefan Wyszyński University, Dewajtis 5, Warsaw, Poland*

*Received January 31, 2003; Revised Manuscript Received May 21, 2003*

ABSTRACT: A small-angle light-scattering (SALS) technique is performed to investigate the phase separation in the films of flexible polymer (polystyrene, PS) mixed with low molecular weight thermotropic liquid crystal LC (4-cyano-4′-*n*-octylbiphenyl, 8CB). The growth of isotropic (polymer) domains is studied in both isotropic and anisotropic (nematic or smectic phase) LC matrices, as a function of time, film thickness, and film composition. The size of the domains, $L(t)$, grows algebraically with time as $L(t) \sim t^{\beta}$. For 70/30 wt % of 8CB/PS, we found the diffusion growth in isotropic ($\beta = 0.25$) and smectic ($\beta = 0.28$) matrices, independent of the film thickness. In the nematic matrix, $\beta$ changes from 0.33 to 0.47 as we change the thickness of the sample from 120 to 10 $\mu$m. We think that the change of $\beta$ is due to the attractive forces between the polymer domains which follow from the elastic deformations of the nematic matrix caused by the glass surfaces and polymer domains. In every matrix and for different thicknesses of a sample, scaling is observed in this growth regime. At longer times, there is a crossover from the diffusion growth to the hydrodynamic fast-mode growth, characteristic for systems in which one of the components wets the confining walls. In this regime, we do not observe the scaling; i.e., there is more than one characteristic length scale in the system, and $\beta$ ranges from 1 to $^3/_2$. Considering extremely viscous systems (50/50 wt % of 8CB/PS), we also find the diffusion growth but with smaller exponent $\beta < 0.2$. In this case, we observe two peaks in the scattering intensity $S(q,t)$. One of them is the surface and one the bulk peak. For systems with small amount of a polymer (90/10 wt % of 8CB/PS), the process of growth is very fast, and $\beta = 0.4$. In this case, the bulk peak is very quickly covered by the peak coming from the growth of the domains at the surface. To perform the measurements in anisotropic LC systems, we had to eliminate the multiple scattering of light coming from the large difference in ordinary and extraordinary refractive indexes of LC.

## I. Introduction

**1. Liquid Crystal/Polymer Mixture.** Inhomogeneous composite materials consisting of liquid crystals and polymers are of considerable current interest for fundamental scientific reasons and because of their very great potential for use in flat displays. Polymer-stabilized liquid crystals (PSLC's) consist of a small amount of polymer dispersed throughout a continuous liquid-crystal phase,[1] while polymer-dispersed liquid crystals (PDLC's) consist of liquid-crystal droplets dispersed in a polymer matrix.[2,3] Both of these materials can be switched between states with different optical properties by modest applied fields, and this property makes them candidate materials for display applications, infrared shutters, angular-discriminating filters, thermo-electrooptic switches, memories, gas flow sensors, optical sensors, and optical gratings etc.[4] The simplest way of preparing such materials might be the thermally induced phase separation obtained by cooling the homogeneous mixture of LCs and thermoplastic polymers below their consolute point.[5,6] The electrooptical performance of those materials depends strongly on the morphology of the phase-separated structure, and this morphology is mainly determined by both the thermodynamics and the kinetics of phase separation during the preparation process. Thus, the understanding of the phase equilibrium and phase separation dynamics of a mixture of liquid crystal (LC) and polymer (P) is of central importance for optimizing the performance of PDLC and PSLC materials.

**2. Phase Separation in Isotropic Systems.** The process of phase separation is usually studied in the binary mixtures (AB) which is quenched below the consolute (critical) temperature into the thermodynamically unstable region (spinodal region) of the phase diagram. In this case, spinodal decomposition (SD) takes place, which manifests in the spontaneous growth of the concentration fluctuations that leads the system from the homogeneous to the two-phase state. Shortly after the phase separation starts, the domains of A and B components are formed, and the interface between the two phases can be specified. There are actually a few different regimes of the separation processes (at least early, intermediate, and late) studied and described in details by Bates[7] and Hashimoto[8] for homopolymer blends.

Early stages of the spinodal decomposition process are described by the linearized Cahn−Hilliard theory.[9−11] After the temperature quench below the spinodal temperature, the system becomes unstable with respect to small fluctuations of wavevector $q$ smaller than some value $q_0$. The key prediction of the theory is the exponential growth of the scattering intensity $S(q,t)$ in time with a well-defined maximum at $q_{max} = q_0/\sqrt{2}$. Interpenetrating A-rich and B-rich domains of the size of $1/q_{max}$ form a bicontinuous structure. At this point the domains mainly saturate; i.e., the scattering is mainly due to the increase in the composition difference between A-rich and B-rich domains. Once the composition inside A-rich and B-rich domains gets saturated, the further coarsening process (growth of the average domain size, $L(t)$ in time $t$) is driven by the interface

[†] Institute of Physical Chemistry PAS.
[‡] Cardinal Stefan Wyszyński University.

10.1021/ma034135b CCC: $25.00 
Published on Web 08/07/2003

curvature.[11] The system at long times finally gets into the late stage growth regime. In the late regime, one finds the power law growth of $L(t)$ and scaling; i.e., a morphological pattern of the domains at earlier times looks statistically similar to a pattern at later times apart from the global change of scale implied by the growth of $L(t)$—the domain size. Quantitatively, it means for example that the correlation function of the A component concentration has the following functional form:

$$g(r,t) = g(r/L(t)) \tag{1}$$

where

$$L(t) \sim t^{\beta} \tag{2}$$

the characteristic length scale in the system, scales algebraically with time $t$ with the exponent $\beta$ depending on the particular dynamic process (i.e., diffusion, hydrodynamic flow, etc.), which governs coarsening.[11] The Fourier transform of the correlation function gives the scattering intensity:

$$S(q,t) = \int \mathrm{d}^d r\, g(r,t) \mathrm{e}^{iqr} \tag{3}$$

where $d$ is the dimension of the system ($d = 3$ for a growth in a bulk 3-dimensional system, $d = 2$ for a growth in 2-dimensional system). This transform can be represented in the following scaling form:

$$S(q,t) = L^d(t) Y[qL(t)] \sim q_{\max}{}^{-d}(t) Y(q/q_{\max}(t)) \tag{4}$$

where $q$ is the scattering wavevector and $Y$ is the scaling function. In general, one uses relation 4 to check the scaling. In practice,[8,12] one determines the location of the maximum of $S(q,t)$, $q_{\max} \sim 1/L(t)$, and the value of $S(q,t)$ at the maximum, $S_{\max}$, to have a quick check of scaling since according to (4)

$$S_{\max}(t) \sim q_{\max}(t)^{-d} \tag{5}$$

If $S_{\max} \sim t^{\alpha}$ and $q_{\max} \sim (t)^{-\beta}$, then scaling implies that $\alpha = d\beta$. In general, when the domains are still not saturated, we expect that approximately

$$S_{\max}(t) \sim \langle \phi(t)^2 \rangle q_{\max}(t)^{-d} \tag{6}$$

where $\langle \phi(t)^2 \rangle$ denotes the composition fluctuations in the domains. Therefore, in principle, one can determine the time scale for the saturation of the domains in the separation process from this formula.

If both phases are isotropic and the growth in a 3-dimensional system ($d = 3$) is induced by simple diffusion, then typically $0.25 < \beta < 0.33$[13,14] while for the growth governed by hydrodynamic flows $1 < \beta < {}^3/_2$.[14−16] In simple liquids, the crossover between the diffusion and hydrodynamic regime is gradual and occurs at $L(t) \approx \sqrt{\lambda_0 \eta}$, where $\lambda_0$ is the transport coefficient and $\eta$ is the viscosity.[11]

**3. Phase Separation in Anisotropic Systems: Theoretical Prediction for a Two-Dimensional System (2D).** While the dynamics of phase separation has been extensively studied in isotropic liquids, little work has been done on equivalent problem in anisotropic liquid systems. Recently researchers started a theoretical study of the growth of isotropic domains in the nematic solvent (or nematic domains in isotropic matrix) for 2d[17,18] and 3d systems.[19]

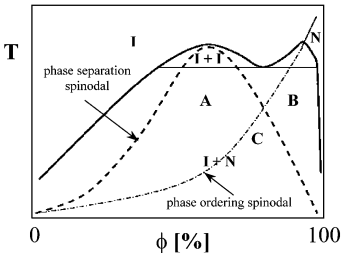


**Figure 1.** Hypothetical phase diagram of two-dimensional rod/coil blend (polymer/nematic liquid crystal mixture) proposed by Lapena et al.[17] $T$ is the temperature in arbitrary units, and $\phi$ is the local area concentration of rods. The heavy solid line is the coexistence curve. The spinodals are the limits of metastability of the isotropic phase. At low temperatures, an isotropic phase rich in polymer coils coexists with a nematic phase of LC rich in rods. "I" and "N" denote an isotropic phase and a nematic phase. Regions A−C indicate various temperature quenches performed at different compositions.

The phase diagram for the mixtures of flexible polymer (P) and thermotropic low molecular weight liquid crystal (LC) was proposed[17] (Figure 1). It is highly asymmetric and exhibits various coexistence regions such as isotropic−isotropic (I + I), isotropic−nematic (I + N), and pure nematic (N) at the high composition of LC.

Under a deep quench (I + N region), the P−LC mixture is separated into an isotropic phase of a polymer and a nematic phase of LC. The demixing region can be further divided into two parts by a phase-ordering spinodal curve. On the left side of this curve, the isotropic phase of LCs is metastable while on the right side it is unstable. According to the assumption of the mean-field theory that ordering is much faster than phase separation, whether the initial homogeneous phase immediately following a sudden quench is in the metastable region of isotropic phase of LC or in the unstable region, is completely determined by the position of the quenched state. There are two spinodal curves, termed as the spinodal curve for phase separation and spinodal curve for phase ordering, which constitute an important characteristic of the P−LC mixture. Therefore, the SD behaviors are different for different concentrations of the system. There is also a big difference in the time scales of separation and ordering. Nucleation of the nematic phase in the metastable isotropic phase can be orders of magnitude faster than the nucleation of polymer domains in the metastable or unstable isotropic solvent.

It has been found[17] that ordering dramatically affects morphology, giving rise, for example, to interconnected networks or elongated domains depending on whether ordering or phase separation is the initially dominant process. The emergence of domains morphology in nematic/polymer composite films can be investigated by means of the optical microscopy, following several thermal quenches from a single phase to various regions of the phase diagram.

**(a) Temperature Quench into the Unstable Liquid−Nematic Region (Quench A).** The point after quench lies below the spinodal for the phase separation and above the one for the ordering. Initially, this quench leads to circular droplets rich in the rods of liquid crystal in a matrix rich in the coils of polymer. When the concentration of rods in the droplets is comparable to the concentration at the phase-ordering spinodal, the

rods in droplets begin to order. At this time, the droplets abruptly expel more coils because the coils are less soluble when the rods are ordered. In addition, the droplets must develop defects because the rods want to be parallel to each other and parallel to the droplet interface. As the rods order, a pair of defects forms inside each droplet and separates, with the two defects moving along the director in opposite directions toward the edge of the droplet. The magnitude of orientational order is lower at the edges than in the center; thus the defects migrate toward the edges to lower their energy. Since the overall system is isotropic, the long axis of each droplet is randomly oriented.

**(b) Temperature Quench into the Metastable Liquid−Unstable Nematic Region (Quench B).** In this region, the system is initially metastable with respect to phase separation, but it is unstable with respect to ordering. The instability toward orientational ordering eventually drives the system to phase separate because the two order parameters are coupled. This makes physical sense; once the rods are strongly aligned, they expel the coils into isolated droplets. Although there is no orientational order within the coil-rich droplets, the droplets are anisotropic because of the nematic elasticity in the surrounding rod-rich matrix.

**(c) Temperature Quench into the Unstable Liquid−Unstable Nematic Region (Quench C).** The system is initially unstable both to phase separation and to ordering, but we can observe a further two cases.

**(i) System More Unstable with Respect to the Phase Separation.** The system forms the bicontinuous network that rapidly breaks up into droplets rich in long coils. However, defects in the surrounding rod-rich domains give rise to droplets that are noncircular. Furthermore, the coupling of phase separation and ordering leads to a faster onset of phase separation because the rod-rich regions tend to expel coils as the rods order.

**(ii) System More Unstable with Respect to Ordering.** Once the degree of order is significant, then phase separation begins. Because of ordering, phase separation begins very early. Small highly ordered rod-rich droplets initially are formed in a coil-rich matrix. As these rod-rich droplets grow, the surrounding coil-rich region shrinks into a network of interconnected domains that are strikingly fibrillar, despite the fact that the coil-rich phase is the minority phase. This is in contrast to system with only a compositional order parameter, where only the majority phase can form networks. Eventually, this network breaks up to form coil-rich droplets; again, these are noncircular because of defects in the surrounding rod-rich regions. In some cases, the cross-linking of the polymer network may arrest the phase separation at the fibrillar network stage.

All these aforementioned predictions concerning morphology are found for the small two-dimensional (2d) systems of size 128 × 128 lattice points[18] or three-dimensional (3d) systems—(64 × 64 × 64) or (32 × 32 × 32) cubic lattices.[19] However, it has been shown recently, for some simple models of growth dynamics in a system of a nonconserved order parameter, that in order to reach the late-stage scaling, the system's size must be much larger than 100 × 100 × 100.[20] The exponents determined in a smaller system are not the late-stage scaling exponents.

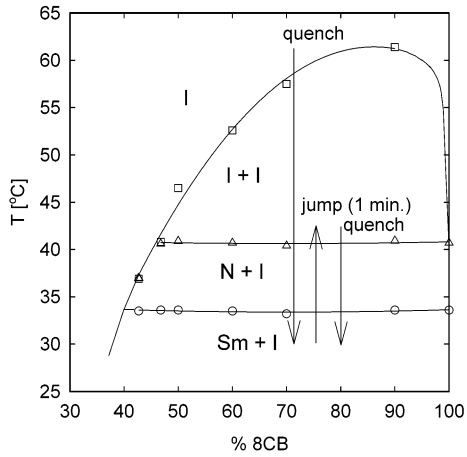


**Figure 2.** Equilibrium phase diagram of PS ($M_w$ = 65 000 g/mol)/8CB: temperature vs the concentration of 8CB. The symbols in this diagram represent experimental data obtained by optical microscopy. Squares represent the transition temperature from isotropic 8CB + isotropic PS (I + I) to homogeneous, isotropic mixture (I), triangles represent the transition temperature from nematic 8CB + isotropic PS (N + I) to isotropic 8CB + isotropic PS (I + I), circles represent the transition temperature from smectic 8CB + isotropic PS (Sm + I) to nematic 8CB + isotropic PS (N + I). To observe the growth of the polymer-rich domains in the ordered (nematic or smectic) matrix, we use the following temperature sequence: quench (0.5 or 1 h) to the ordered phase from the one-phase region → jump to the isotropic phase (1 min) → quench back (see also text for explanation of the multiple scattering of light). The samples were annealed at $T$ = 60 °C and quenched into the nematic (39 °C) or smectic phase (32 °C) of LC. The jump was made to $T$ = 41 °C for both cases. Most of the measurements were performed for 70/30% of 8CB/PS by weight. Some of them were performed for concentrations 50/50% and 90/10% of 8CB/PS.

There are no theoretical predictions for the growth of isotropic domains in the positionally ordered (smectic) matrix.

We are aware of only few experimental measurements,[21−23] complementary to our studies, of the growth exponents in anisotropic media. Casagrande et al.[21] observed an anisotropic diffusion growth in the nematic−nematic phase separation under the microscope for the mixture of liquid crystalline polymer and low molecular weight liquid crystal. The determined exponent was 0.33 ± 0.03. Roux and Knobler studied[22] the isotropic−lamellar phase separation in the mixture of surfactant, cosurfactant, water, and oil. The authors found for the system size $h$ = 400 $\mu$m and $\beta$ = 0.33 ± 0.06, but the close inspection of their Figure 4 indicates that they also see (although they do not interpret) the crossover to the hydrodynamic regime. There were also studies of the phase separation in the system of polymer and liquid crystal in the nematic phase, e.g. ref 23. Here, the time evolution of structure factor reveals a crossover of a kinetic exponent $\beta$ from 0.33 to 0.6 or larger. We note however that the study of separation in nematics is plagued by the multiple scattering of light, which precludes the interpretation of data in terms of two-body correlation function. To interpret the data, the multiple scattering has to be eliminated.

*It is the purpose of this paper to determine experimentally the phase separation in the system in which one of the phases is anisotropic, with or without positional ordering and determine the growth exponents.* We take as a paradigm of such a system a mixture of polymer and liquid crystal which exhibits phase separation both

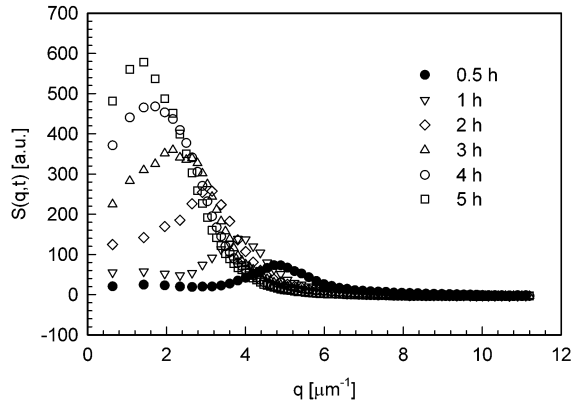


**Figure 3.** Scattering intensity $S(q,t)$ after a quench from a high temperature (60 °C) to the I + I region (41 °C) as a function of the wavevector $q$ for different times. The measurement was taken for concentration 70/30% of 8CB/PS by weight. It shows the known behavior during the spinodal decomposition. The peak grows and its location shifts toward smaller wavevectors, indicating the growth of the average size of the PS-rich and 8CB-rich domains (coarsening process).

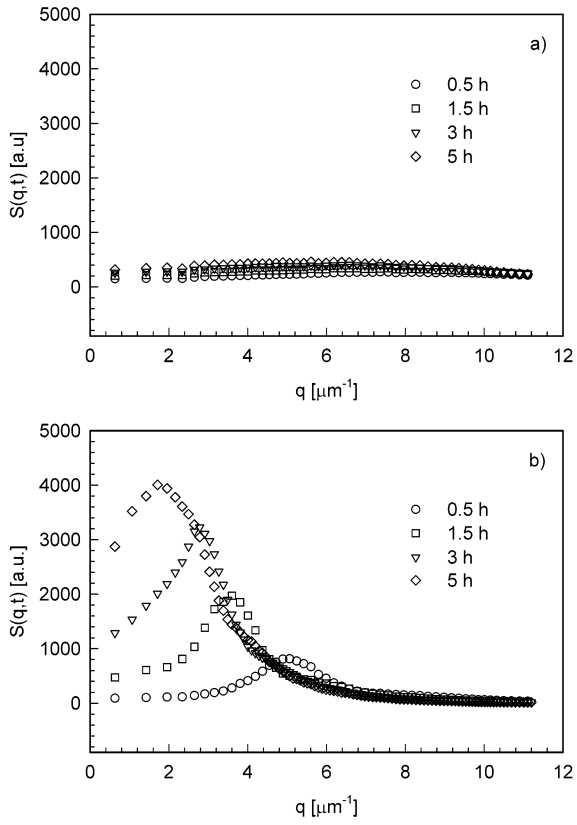


**Figure 4.** Scattering intensity $S(q,t)$ vs the scattering wavevector for different times during the growth process in the N + I region, for the thickness of the sample $h = 120$ $\mu$m, showing the effect of the multiple scattering of light. The concentration was 70/30% of the 8CB/PS by weight. (a) Flat curves are the scattering data taken directly in the nematic phase (39 °C). In this region the peak is hidden under multiple scattering background. (b) The curves with a large peak are the data taken after jump to the isotropic phase (41 °C). The change of contrast after the jump between 8CB/PS revealed the structure of the polymer domains in the system.

in the nematic and smectic phases and study it by the small-angle light scattering (SALS).

The recent study of suspensions of small oil or water droplets in anisotropic solvent revealed strong attractive forces between the droplets induced by the elastic deformation of the anisotropic medium.[24−26] We would also like to see how the elastic forces affect the growth process of isotropic phase in the anisotropic matrix.

**4. Interactions between Isotropic Inclusions in the Anisotropic Matrixes.** If we distort the nematic or smectic medium, it responds elastically due to the orientational and/or positional order, respectively. The important role in the formations of these distortions are the conflicting boundary conditions. For example, if we put a spherical inclusion,[27] in the planar nematic, with the homeotropic (perpendicular) boundary conditions at the surface of the sphere, we get characteristic deformations with disclination ring in the proximity of the surface. Two such spheres will attract each other at large distances because grouping them together reduces the total distortion in the nematics medium. At short distances, the spheres would strongly repel each other, because of the defects.

Recently, some very careful measurements have been done for the elastic forces in the well aligned nematic liquid crystal (with the orientation of molecules parallel to the glass plates).[28] The authors mixed their liquid crystal with the water droplets and obtained an emulsion of water droplets suspended in the nematic matrix. The orientation of the LC molecules on the surface of the droplets could be either planar (for water with a special surfactant) or perpendicular (homeotropic). In all cases the anchoring was strong enough to induce the distortions in the nematic matrix. A very simple estimate of the total energy of such distortions can be made on the basis of the Franck elastic energy for nematics.[28] The energy associated with the deformation is given by $E = KR$, where $K$ is the nematic elastic constant and $R$ is the radius of the droplet. Typically $K = 10^{-11}$ N and $R = 1$ $\mu$m, which gives $E$ on the order of $1000k_\beta T$. It means that in the free energy the entropic part is negligible in comparison to the elastic interactions. In the case of homeotropic alignment of LC molecules at the surface of the droplets, the water spheres attract each other at large distance with the dipolar forces given by $AR^4/r^4$ and repel each other at short distances (on the order of $2.5R$). As a result, water droplets form linear chains, with the distance between droplets roughly equal to $2.5R$. In such geometry, the droplets do not touch one another. The careful observation of the nematic structure close to the surface of the droplets revealed the formation of topological defects called hyperbolic hedgehog defects. They are responsible for the repulsive interaction at short distances between droplets. A different situation is observed with the planar anchoring at the surface of water droplets. In this case, the droplets attract each other and come into close contact forming large aggregates. The aggregates last for few minutes and then undergo a quick coalescence. It indicates that there are no repulsive interactions at short distances.

In our experiment, we put the LC sample between the glass plates. The plates prefer planar orientation; however, no special treatment of the plates is done (rubbing, coating with surfactants, etc.). Therefore, we have planar random orientation on the plates. We have observed the characteristic Schlieren texture, which indicates planar imperfect ordering.[29] Moreover, during the phase separation the polystyrene (PS) domains start to grown in the nematic matrix. The orientation of the LC molecules on the PS surface is almost planar with the tilt angle from the normal to the surface of 72°.[30]

Therefore, our situation is close to the one described by Poulin and Weitz,[28] although we do not have a global planar alignment in the sample, but instead we have many planar domains of different orientations and defects. It suggests that we can expect the attractive interactions between the PS domains and their further coalescence induce by these forces. A priori, we cannot tell what is the interaction potential between the PS spheres in the nematic or smectic matrix, because it depends in a complicated way on the orientations of LC domains.

There have been some studies of the large inclusions in smectic films.[31] The authors found experimentally that the interaction between spherical inclusions in the smectic layers (smectic C*) is attractive at large distances and repulsive at short distances preventing the inclusions to coalesce.

Summarizing: the elastic interactions between the inclusions in the anisotropic matrices can have a long-range attractive part and a short-range repulsive part. In some special orientations of the nematics matrix (planar orientation), the repulsive part is absent and the attractive part can induce coalescence of inclusions.

This paper is organized as follows: First, in section II, the samples, experimental methods, and phase-separation conditions are described. In this section, we present also the phase diagram of PS/8CB. In section III, the multiple scattering is characterized and we show here the method of its elimination. Experimental results of the growth of the polymer domains in isotropic, nematic and smectic matrices of liquid crystalline material will be presented in section IV. A test of the scaling postulate will also be discussed here for different compositions of a mixture. The whole results of our experiment are summarized in section V.

## II. Experimental Section

**(a) Sample Description.** We have used a mixture of polystyrene (PS) from Fluka Chemical Co. characterized by, $M_w = 65\,000$ and $M_w/M_N = 1.02$ and a liquid crystal 4-cyano-4′-*n*-octylbiphenyl (8CB). The index of refraction ($n$) of PS we have from Fluka tables, $n_{PS} = 1.589$, and $n$ of 8CB was measured by us in a refractometer. In the isotropic phase $n_{8CB} = 1.566$, so $\Delta n = 0.023$. Most of the measurements were done for 30/70 wt % for PS/8CB. Additionally we have done some measurements in the isotropic phase for 10/90% and 50/50% composition.

**(b) Sample Preparation.** 8CB and PS were dissolved in toluene. The resulting mixture was stirred mechanically overnight. Thin films were prepared by casting from 20% toluene solution on a glass of size 1 cm in diameter. The films were dried at high temperature (60 °C) for 2 days and next were covered by the second glass plate. For microscopic measurements, we did not control the thickness, and for light scattering measurements, the distance between the plates was set by the spacer of known thickness $h = 10$, 50, 120 $\mu$m.

**(c) Optical Microscope Measurements.** The thermomicroscopy studies were performed to obtain the phase diagram of PS/8CB on an optical polarizing microscope Nikon ECLIPSE E 400, equipped with a heating/cooling stage LINKAM THMS 600. Samples were first annealed at high temperature (60 °C) in the homogeneous state for about 2 h. Second, by cooling the sample, we studied the textures of the system. Some measurements for the large fraction of polymer took two or 3 days to determine the I + I regions. The appearance of N order or Sm order was immediate. The measurements were done for six compositions of 8CB/PS (42/58, 46/54, 50/50, 60/40, 70/30, and 90/10 wt %) and for pure 8CB.

Figure 2 presents the equilibrium phase diagram of the PS/8CB mixture. The diagram indicates upper critical solution temperature shape, and it is asymmetric. There are three phase transition lines separating four different regions that are clearly identified on the diagram. One observes a region containing a single homogeneous isotropic phase (I) and three regions where two phases are at equilibrium: isotropic−isotropic (I + I), nematic−isotropic (N + I) and smectic−isotropic (Sm + I). The phase diagram exhibits a large I + I miscibility gap for the investigated molecular weight of PS. The temperatures ranges of N + I and Sm + I are mainly restricted by the phase transition temperatures, isotropic−nematic and nematic−smectic in pure liquid crystal, respectively.

**(d) Light Scattering Measurements.** The scattering of light is monitored on a linear array of 512 photodiodes, and the scattering intensity $S(q,t)$ is determined as a function of the scattering wavevector $q$ and time $t$. The scattering angles, $\theta$, which are accessible in this experiment are 0.5−42°, and the corresponding wavevectors ($q = 4\pi n/\lambda \sin \theta/2$) are 0.2−11 ($1/\mu$m). It means that in the real space we can observe the domains of size $L = 2\pi/q$ between 0.5 and 30 $\mu$m (in principle). In practice, the first few photodiodes are too close to the main beam to give reliable results, and therefore in practice the range of $L$ that can be observed in our apparatus is between 0.5 and 5 $\mu$m. We use the standard laser (He−Ne, 5 mW) of $\lambda = 632.8$ nm and a parabolic mirror to reflect the scattered intensity toward the array of photodiodes. The temperature was controlled up to 0.01° and the typical time for the stabilization of the temperature after a sudden change (even by 10−20°) was 50 s. The parameters of phase separation, intensity of scattered light $S$, scattering wavevector $q$, time $t$, and temperature $T$, were simultaneously registered every 5 s during the heating, and this interval time was adjusted between 5 and 60 s, depending on how fast was the process during cooling.

The samples were first annealed at high temperature (about 60 °C) in the homogeneous state for several hours and then quenched to the one of the regions of the phase diagram (I + I, N + I, or Sm + I), where they were allowed to demix until the peak did not leave the region of wavevectors accessible in our experiment. In the case of N + I or Sm + I, the data for analysis were taken every 0.5 h (after a temperature jump to I + I region for 1 min) because of the multiple scattering (see section III).

## III. Method of Elimination of Multiple Scattering

The study of phase separation in liquid crystal (LC) matrices by SALS has been hampered by the strong anisotropy of the refractive index for ordinary and extraordinary rays passing through the sample. The domains in LC of different orientation, which form in the unoriented samples, lead to very strong multiple light scattering[32−35] because the typical difference in the refractive index for parallel and perpendicular orientation is $\Delta n \approx 0.2$. The mean free path of light in the sample is $l_a = 1/(\sigma\rho)$, where $\sigma \sim (\Delta n)^2$ is the scattering cross-section and $\rho$ is the number density of scattering objects (domains). In the simplest case of Rayleigh scattering, with domains of size 0.1 $\mu$m, the wavelength of red light 0.6 $\mu$m, and 50/50 volume fraction, one finds $l_a \sim 10$ $\mu$m. For the sample size $h \geq l_a$, the multiple scattering effects preclude the simple analysis of the scattering intensity based on a single scattering event (see eq 3). In our experiments, we have used the samples of thickness ranging from 10 to 120 $\mu$m, and therefore in order to observe the coarsening process in SALS, we had to eliminate the multiple light scattering.

As we have mentioned earlier the difference of index of refraction for PS and 8CB in the isotropic phase is $\Delta n = 0.023$, and a very simple estimate[36] gives us the mean free path of light $l_i \sim 10^3$ $\mu$m. We have $l_i \gg h =$

10−120 $\mu$m ≥ $l_a$. Thus, we do not have the multiple scattering in the isotropic matrix, but we do have it in the anisotropic matrix. The idea of the elimination of the multiple scattering of light is based on the observation that the formation of the smectic or nematic order between polymer-rich domains is immediate (on the order of micro- or milliseconds) while the growth of polymer domains occurs on the time scale of minutes or even hours. Our method consists of the following steps (Figure 2): the well-annealed system is quenched to the nematic or smectic phase. It evolves for 0.5 or 1 h, and then we make a temperature jump to the isotropic phase for 1 min, take the measurements of $S(q,t)$, and quench it back to the original temperature in the anisotropic phase. The steps are repeated until the peak of $S(q,t)$ moves outside the available range of $q$ (11 $\mu m^{-1} > q > 0.2$ $\mu m^{-1}$). We study the phase separation for composition 70/30 wt % of 8CB/PS in the I + I (at temperature $T = 41$ °C), N + I ($T = 39$ °C), and Sm + I ($T = 32$ °C) regions of the phase diagram.

In Figure 3, we show the standard and well-known result for the I + I region of increase of the scattering intensity, signaling the phase separation, and the shift of the peak position toward smaller wavevector, signaling the process of coarsening. So we see an evident peak, which demonstrates that there is no multiple scattering when the isotropic domains of polymer grow in time in the isotropic matrix of liquid crystal. On the contrary, Figures 4a and 5a show $S(q,t)$ in the nematic and smectic phase, respectively, before the temperature jump to the isotropic phase for thickness 120 $\mu$m. We see that $S(q,t)$ in the nematic and smectic phase is isotropic (flat curve), indicating that multiple scattering on nematic or smectic domains of different orientation (large contrast) is dominant. After the jump, the anisotropic domains turn into isotropic domains, multiple scattering disappears and a peak coming from the weak 8CB/PS contrast emerges (Figures 4b and 5b). Because the dynamics of the polymer growth is slow, the short jump (1 min) does not change the polymer domains but still allows taking the measurement (taken every 5 s). The peak in $S(q,t)$ coming from a weak contrast between 8CB/PS domains is significant, but in the N + I or Sm + I region, this peak is hidden under the multiple scattering background. We have checked this hidden peak on three different thicknesses of the sample, $h =$ 10, 50, and 120 $\mu$m. We found that when the thickness increases, the covering of the peak is bigger. We have carefully checked that after the second quench the scattering intensity comes back to its original value observed before the jump and to its original shape and size. These results of light scattering were confirmed by the direct optical microscopic observation. We carried out the experiment using the method presented in Figure 2. Optical micrographs of morphology of 8CB/PS blend with composition 70/30 wt % after several cycle of cooling/heating process are shown in Figure 6. The micrographs (Figure 6a−c and Figure 6d−f) for nematic and smectic matrix, respectively, are taken from the same area. The micrographs in Figure 6a (nematic) and Figure 6d (smectic) show isotropic domains dispersed in anisotropic matrix after quench to 39 or 32 °C and after 6 or 379 h, respectively, for nematic and smectic matrices. Then we make temperature jump to 41 °C for 1 min. At this temperature, the liquid crystal turns from the nematic (or smectic) to the isotropic phase, and we observe the isotropic domains dispersed in the isotropic matrix (micrographs in Figure 6, parts b and e). In the next step we make reentry quench to original temperature in the anisotropic phase, 39 (nematic) or 32 °C (smectic). The morphology is shown in micrographs in Figure 6, parts c and f, for nematic and smectic matrices, respectively. As we can see the morphologies before and after the temperature jump are identical, micrographs in parts a and c of Figure 6 for the nematic matrix and parts d and f of Figure 6 for the smectic matrix, respectively. These micrographs confirm that temperature jump to I + I region for 1 min does not influence the morphology of system during the phase separation process in the N + I or Sm + I region. As we have already mentioned, it is due to the separation of time scales: a time scale for ordering (microseconds) and a time scale for growth of polymer domains (hours).

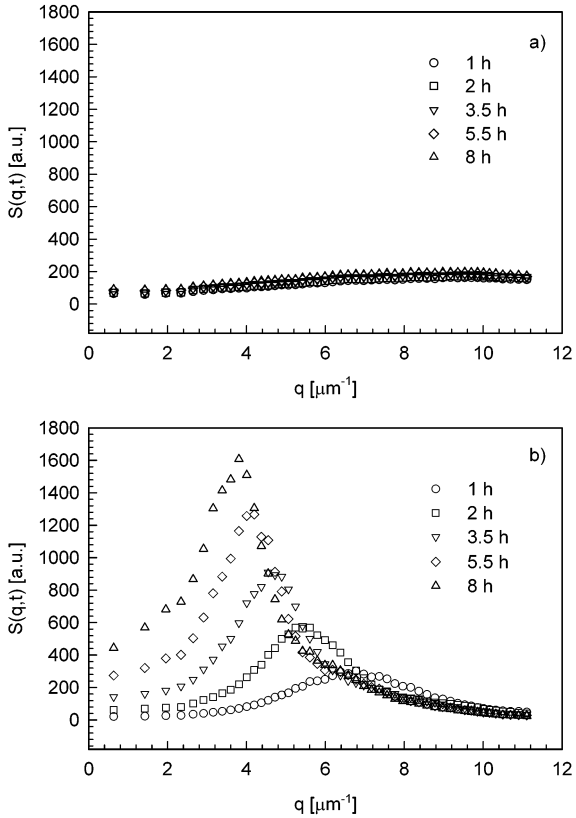


**Figure 5.** $S(q,t)$ in the Sm + I region for the $h = 120$ $\mu$m for 70/30% (8CB/PS) by weight. (a) Data taken in the smectic phase (32 °C). (b) Data taken after jump to the isotropic phase (41 °C).

We have also verified that the same growth laws are obtained if we let the system evolve for 2, 1, or 0.5 h between the temperature jumps or if we do a one-point run.

## IV. Results and Discussion

**Growth Laws. Concentration of the Sample 70/30 wt % 8CB/PS.** The average size of the polymer domains in the I + I region is given by the peak position $L(t) \sim 1/q_{max}(t) \sim t^{\beta}$. In Figure 7a we show the change of the peak position $q_{max}$ as a function of time for three thicknesses of the sample (10, 50, 120 $\mu$m). In the first stage of the growth of the domains, the exponent in all three cases is 0.25 ± 0.02 indicating the growth governed by diffusion. Then we observe a crossover to the

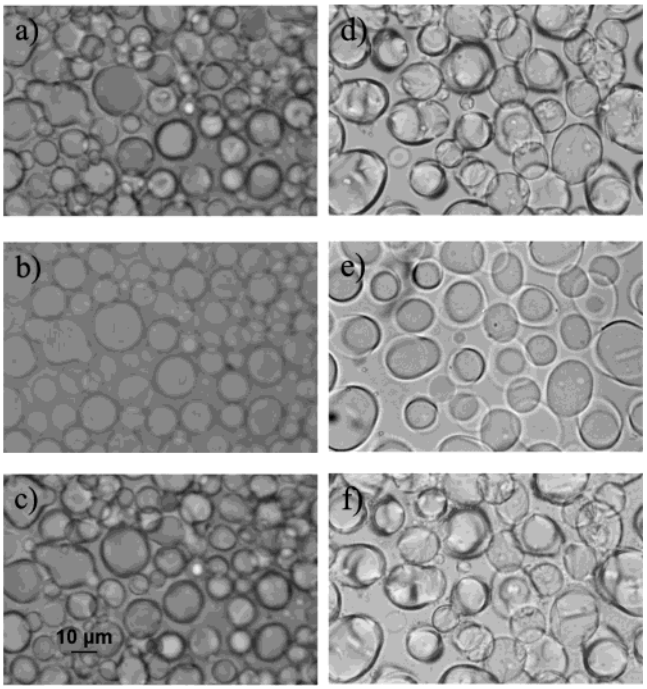


**Figure 6.** Optical micrographs showing the phase separation of the 8CB/PS blend (70/30 wt %) during the quench/jump process. The micrographs show the morphology after (a) quench from the I region (60 °C) to the N + I region at temperature 39 °C after 6 h of phase separation, (b) temperature jump to the I + I region, $T = 41$ °C, for 1 min, (c) reentry quench to the N + I region (39 °C), (d) quench from the I region (60 °C) to the Sm + I region at $T = 32$ °C after 379 h, (e) temperature jump to the I + I region, $T = 41$ °C, for 1 min, and (f) reentry quench to the Sm + I region (32 °C). As we can see the morphologies before and after temperature jump, micrographs a and c for the nematic matrix and d and e for the smectic matrix are identical, respectively. One can observe the same shape of domains dispersed in nematic and smectic matrix, respectively. The size bar of 10 $\mu$m is the same for all micrographs and is shown in micrograph c. Micrographs a−c and d−f, respectively, are obtained from the same area.

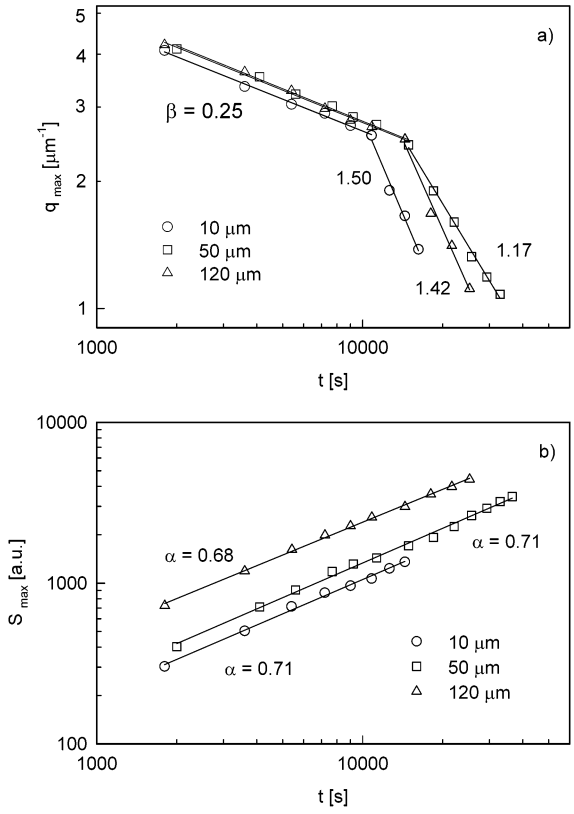


**Figure 7.** (a) Change of the location of the maximum of the scattering intensity, $q_{max}$ as a function of time $t$ on a log−log plot, after quench to the I + I region (41 °C) for three different thicknesses of the sample, for 70/30% of the 8CB/PS by weight. It is shown the crossover from the diffusive to the hydrodynamic growth regime. (b) Change of the maximum of the scattering intensity $S_{max}$ as a function of time $t$ on a log−log plot, for the same conditions as in part a.

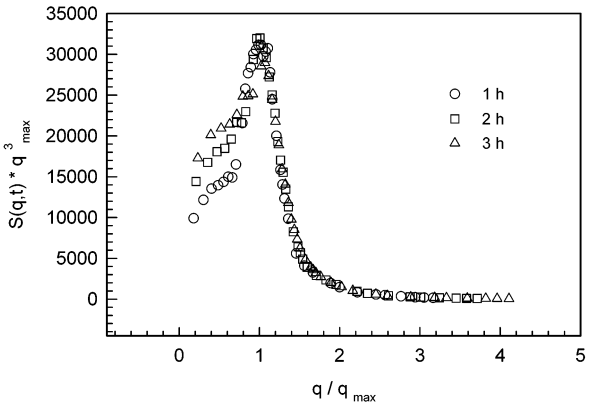


**Figure 8.** Scaling function $Y(q/q_{max}) = q_{max}^3 S(q,t)$ for the growth process in the I + I region for $h = 50$ $\mu$m (the same quality of the scaling function is obtained for all $h$) for 70/30% (8CB/PS) by weight. The scaling is obeyed for the first growth regime, i.e., the diffusion regime with the exponent $\beta = 0.25 \pm 0.02$.

hydrodynamic regime[15] with exponent $\beta = 1.5 \pm 0.3$. The exponent $^3/_2$ suggests the strong wetting conditions[16] for the LC. The sharp crossover between the diffusion and hydrodynamic limited growth is consistent with the computer simulation of binary mixture in a confined geometry under the condition that one of the phases wets the confining walls.[37] In Figure 7b, we show the change of the height of the peak (the average scattering intensity) $S_{max}$ as a function of time for three thicknesses of the sample. We found that the growth of the peak is algebraic with exponent $\alpha = 0.70 \pm 0.05$ in all three cases, in the diffusion regime. Therefore, the scaling $\alpha = 3\beta$ is obeyed in this case (see eqs 1−6). Moreover, in Figure 8 we have plotted $S(q,t)$ $q_{max}^3$ vs $q/q_{max}$, which shows a perfect scaling for all $q$ (not only the $q_{max}$ and $S_{max}$) apart from the very small wavevectors. This lack of scaling for small $q$ can also be explained[37] by the fact that after a quench the wetting layer, which forms at the walls, does not follow the bulk scaling. So we can say that the scaling is satisfied in the diffusion growth process but fails completely in the fast hydrodynamic growth regime.

In the smectic phase shown in Figure 9, the two regimes with exponent $0.28 \pm 0.02$ and $\beta = 0.9 \pm 0.2$ are clearly visible. The latter exponent is characteristic for the fast mode hydrodynamic regime[15] and suggests that the smectic weakly wets the glass.[16] Please note that the crossover to the hydrodynamic regime occurs for the same size of domains in the smectic (inset in Figure 9) and isotropic (Figure 7a) matrices despite the fact that the average shear viscosity of the smectic matrix (10 P) is 1000 times larger than the viscosity in the isotropic matrix ($10^{-2}$ P). In the simplest version of the diffusion growth, the crossover occurs at $L(t) \approx \sqrt{\lambda_0 \eta}$, where $\lambda_0$ is the transport coefficient proportional to the diffusion coefficient $D \sim 1/\eta$, i.e., consistent with our observations. Moreover, the time scale of the

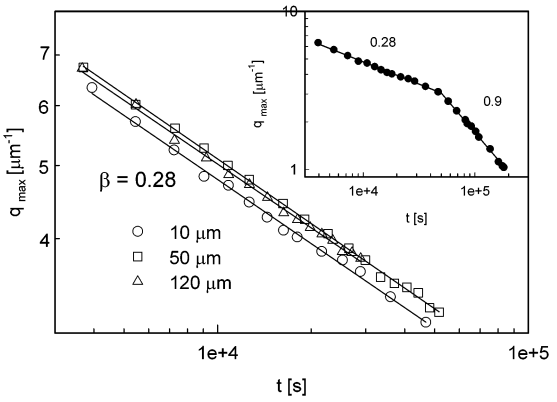


**Figure 9.** Change of the location of the maximum of the scattering intensity $q_{max}$ as a function of time $t$ on a log−log plot, obtained by the method described in Figure 2, for the Sm + I region for three different thicknesses of the sample for 70/30% of the 8CB/PS by weight. In the inset, the crossover to the hydrodynamic growth regime is shown for 10 $\mu$m.

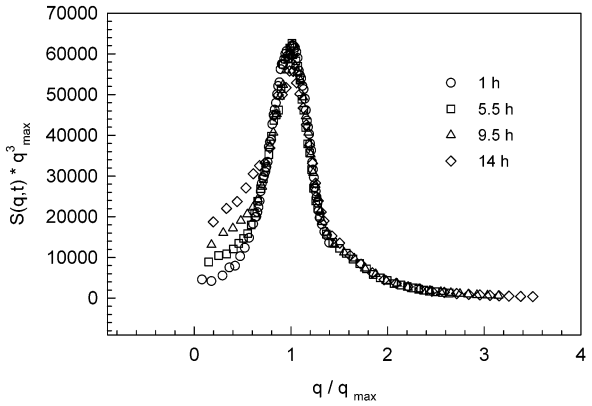


**Figure 10.** Scaling function $Y(q/q_{max}) = q_{max}^3 S(q,t)$ for the growth process in the Sm + I region for $h = 50$ $\mu$m for 70/30% (8CB/PS) by weight. The scaling is obeyed for the first growth regime, i.e., the diffusive regime with the exponent $\beta = 0.28 \pm 0.02$

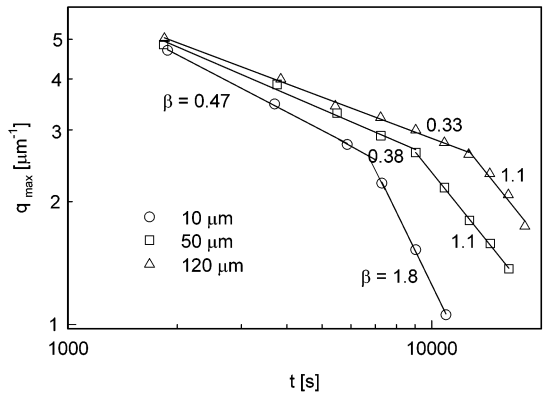


**Figure 11.** Change of the location of the maximum of the scattering intensity, $q_{max}$, as a function of time $t$ on a log−log plot, for the N + I region for 70/30% of the 8CB/PS by weight. Here the exponent $\beta$ depends on the film thickness.

crossover[11] seems to scale as $(\eta)^{1/3}$, and for the smectic, it occurs at times 1 order of magnitude longer than that for the isotropic matrix (Figure 7a and inset of Figure 9). The scaling is satisfied in the diffusion growth process (Figures 8 and 10) but fails completely in the fast hydrodynamic growth regime both in the isotropic and smectic phases. The scaling phenomena is also obeyed for another thicknesses of the sample—10 and 120 $\mu$m for the smectic phase.

The nematic does not conform to the diffusion-limited growth (Figure 11). Moreover, the growth exponent depends on the thickness of the sample. It changes from $\beta = 0.33 \pm 0.03$ to $\beta = 0.47 \pm 0.03$ as we change $h$ from 120 to 10 $\mu$m. Despite the fact that the exponent in the early regime changes with the thickness of the sample, the scaling is obeyed. We believe that the elastic forces especially for thin samples govern the growth in the nematic matrix. Let us make the simple estimate of the growth exponent in the case of elastic forces acting on polymer domains in the spirit of the article by Siggia,[14] i.e., for the droplets. Two droplets of size $L(t)$, separated by the distance $r$, attract each other with the force $F(r, L(t))$; i.e., the force depends on the size of the droplets.[25] Under the influence of the force $F$, the distance between two droplets $r$ changes according to the well-known Stokes equation

$$\frac{dr}{dt} = \frac{F(r,L(t))}{\eta L(t)} \tag{7}$$

where $\eta$ is the viscosity of the medium.

If we average this equation, we find the evolution for the average distance between droplets. Assuming $\langle F(r,L(t))\rangle \approx F(\langle r\rangle, L(t))$, we have

$$\frac{d\langle r\rangle}{dt} = \frac{F(\langle r\rangle, L(t)))}{\eta L(t)} \tag{8}$$

Because our system exhibits scaling, it means that there is only one length scale in the system $L(t)$, and thus $\langle r\rangle$ must be also proportional to it; i.e.

$$\langle r\rangle \approx bL(t) \tag{9}$$

where $b$ is a constant.

Moreover, from Poulin and Weitz[28] and according to scaling eq 1, we assume

$$F(r,L(t)) = \tilde{F}\left(\frac{r}{L(t)}\right) \tag{10}$$

Putting (9) and (10) into (8), we find

$$b\frac{dL(t)}{dt} \approx \frac{\tilde{F}(b)}{L(t)\cdot\eta} \tag{11}$$

Solving this equation, we find

$$\frac{1}{2}(L(t))^2 = \frac{\tilde{F}(b)}{b\eta}t \tag{12}$$

from which it follows the exponent $\beta = 0.5$ and $L(t) \sim t^{0.5}$.

The exponent 0.47 for $h = 10$ $\mu$m is consistent with our prediction. From the measurement of the growth exponent, we conclude that there is a crossover in nematics from the diffusion growth for large thickness of the sample to the growth governed probably by the elastic forces for small size of the system. It means that the strength of the attractive force between the polymer domains induced by the deformation of the nematic matrix increases with the decreasing thickness of the sample. In thin samples, the deformations of the director are very large in comparison to thick samples (distances are smaller and thereby the gradients are larger). That is why the elastic forces are more important in very thin samples.

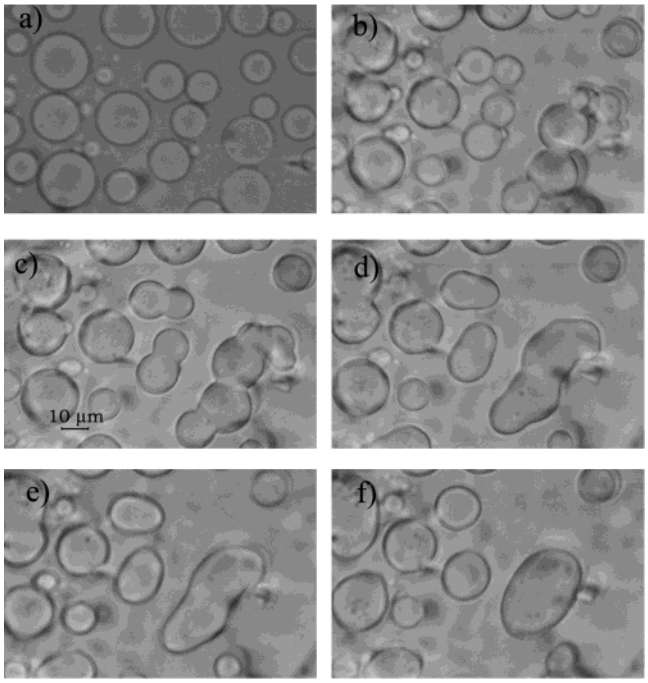


**Figure 12.** Optical micrographs of the phase separation of the 8CB/PS blend (70/30 wt %). (a) Morphology after quench from the I region (60 °C) to the I + I region (temperature 41 °C) after 18 h. (b−f) Time evolution of the phase separation process after second quench to the N + I region (39 °C) in the (b) $t = 2$ min, (c) $t = 3$ min, (d) $t = 6$ min, (e) $t = 9$ min, and (f) $t = 20$ min, $t$ is the time spent after the second quench. These micrographs are obtained from the same area. Micrographs b−f show how fast the isotropic domains surrounded by the anisotropic phase (nematic) merge. The size bar of 10 $\mu$m is the same for all micrographs and it is shown in micrograph c. In the isotropic phase, the domains stayed close together for hours without coalescence, while in the nematic phase the same domains merge in a short time of minutes. Therefore, we suppose that there must be an attractive force in the nematic which pulls the domains together.

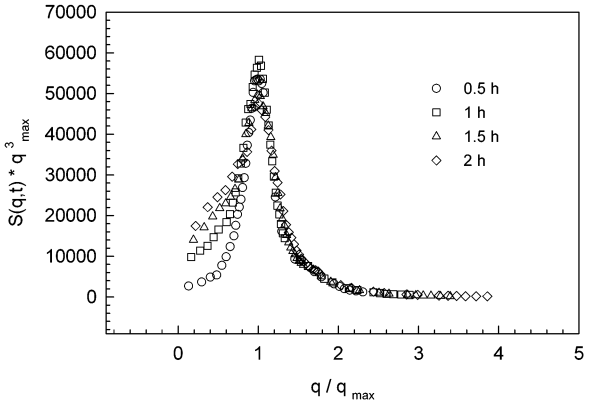


**Figure 13.** Scaling function $Y(q/q_{max}) = q_{max}^3 S(q,t)$ for the growth process in the N + I region for $h = 50$ $\mu$m for 70/30% (8CB/PS) by weight. The scaling is obeyed for the first growth regime irrespective of the thickness of the sample.

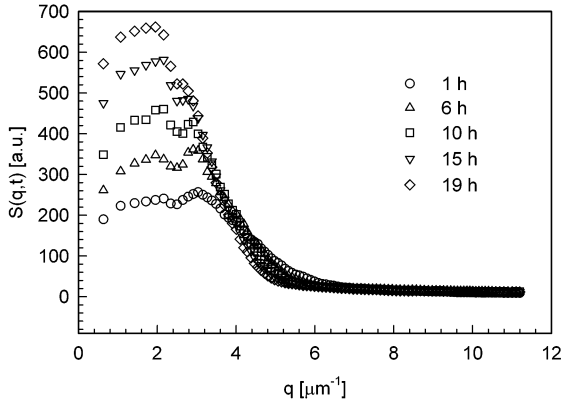


**Figure 14.** Scattering intensity $S(q,t)$ vs the scattering wavevector $q$ for different times during the growth process for the mixture 50/50 wt % of the 8CB/PS, in the I + I region, for the thickness of the sample $h = 50$ $\mu$m. Two distinct peaks are clearly visible.

To verify that there are some attractive forces between the polymer domains in the nematic matrix, we have made the following experiment using optical microscope. In Figure 12, we show the micrographs, which were taken during the phase separation of 8CB/PS blend (70/30 wt %). In direct optical microscopic observation the system is first allowed to decompose spinodally at 41 °C in the isotropic region (I + I) for 18 h (micrograph in Figure 12a). We have not observed any rapid coalescence of droplets in the isotropic phase. In this micrograph, we see large, well-developed isotropic circular droplets dispersed in the isotropic matrix. Then we make the second quench to 39 °C to the N + I region. Time evolution of the phase separation process after the second quench is shown in micrographs in Figure 12b−f. We can see the rapid process of joining isotropic droplets into larger domains surrounded by the nematic phase. The nearest droplets connect each other (micrograph in Figure 12b) and the isotropic domains became more elongated (micrographs in Figure 12c−e) with lapse of time. After 20 min, the shape of domains change from elongated to more circular (micrograph in Figure 12f), and after 40 min (not shown here), they become much larger, some of them with a diameter greater than 20 $\mu$m. Such a rapid coalescence of droplets in the nematic phase can only be possible if the droplets are pulled together after the appearance of the nematic order.

It is interesting to note that the growth exponent in the hydrodynamic regime for very thin films is larger than $^3/_2$, although we note that there is nothing universal (no scaling) in this regime. We cannot explain such a large exponent by the existing theories. The fast mode hydrodynamic crossover originates from the wetting layer. The scaling is obeyed only for the dynamic regime (Figure 13).

We have verified that one can discern two peaks in $S(q,t)$ in the isotropic, nematic, and smectic matrices, one at short wavevectors and one at large wavevectors. The peak at short wavevectors is due to the large domains forming at the surface (wetting layer). The peaks are much better visible for very thin samples (10 $\mu$m). Such behavior seems to be universal for mixtures in which one of the components wets the wall.[15]

**Concentration of the Sample 50/50 wt % 8CB/PS.** For 50/50 wt % samples, we have observed a different behavior in the isotropic phase. From the beginning of the process, we can observe two distinct peaks on the plot $S(q,t)$ vs $q$, both at short wavevectors (Figure 14). It means that the process of phase separation starts both at the surface of the sample (2d) and in the bulk (3d); moreover, the large domains appear very fast (few minutes). Domains grow very slowly without being saturated for a long time. So the samples are very transparent with weakly saturated large domains. After saturation (about 13 h) the process of growth is alge-

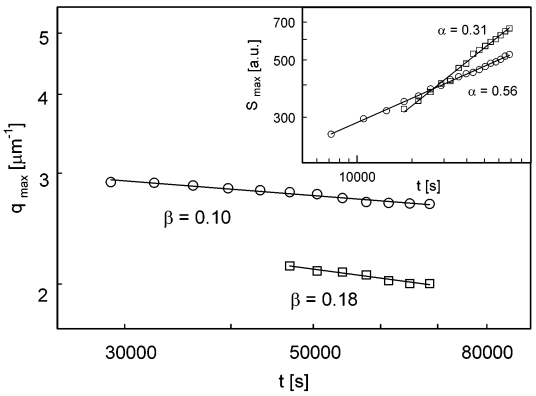


**Figure 15.** Change of the location of the maximum of the scattering intensity $q_{max}$ as a function of time $t$ on a log−log plot, for the I + I region (41 °C) for thickness of the sample $h = 50\ \mu$m for 50/50 wt % of the 8CB/PS. The process of growth is concerned here separately for each of the peaks. Inset: change of the maximum scattering intensity $S_{max}$ in time $t$ on a log−log plot, for those two peaks.

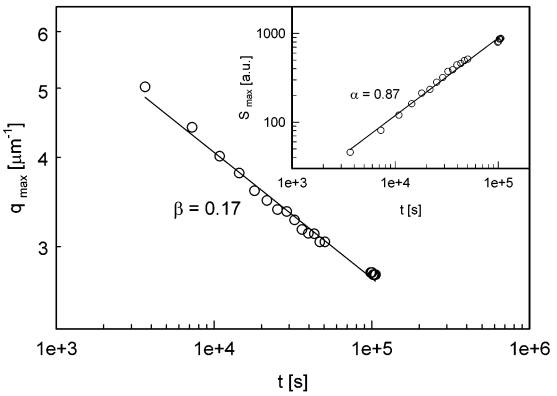


**Figure 16.** Change of the location of the maximum of the scattering intensity $q_{max}$ as a function of time $t$ on a log−log plot, for the N + I region (39 °C) for the thickness of the sample $h = 50\ \mu$m for 50/50 wt % of the 8CB/PS. The results are shown only for larger wavevectors (small domains). Inset: the change of the maximum scattering intensity $S_{max}$ in time $t$ on a log−log plot indicates the algebraic growth.

braic. Characteristic exponent of growth for smaller domains (larger wavevectors) $\beta = 0.10$, and for larger domains (smaller wavevectors) $\beta = 0.18$ (Figure 15) and the scaling is not obeyed. In both cases, the exponent is much smaller than a typical growth exponent governed by diffusion (typically $0.25 < \beta < 0.33$). Our results suggest that for extremely viscous system the growth exponent governed by diffusion can be smaller than 0.25.

In the nematic phase shown in Figure 16, the growth is also algebraic, and still the system does not exhibit scaling phenomena. We analyzed only the first peak (at larger wavevector) because the measurements lasted too short (15 h) to obtained clearly visible second peak. Furthermore, we noticed that after the quench the scattering intensity at first increases and then slowly decreases to the value that was registered before the jump. Most likely, it is caused by the viscoelastic forces. The viscosity of a smectic matrix is too large to perform measurements in a reasonable time.

We see that the process of growth of the domains in the system of concentration 50/50 wt % is not similar to that one for 70/30 wt %. Most likely, different behavior is caused by the different morphology of the system and the large disparity in the viscosity of both components.

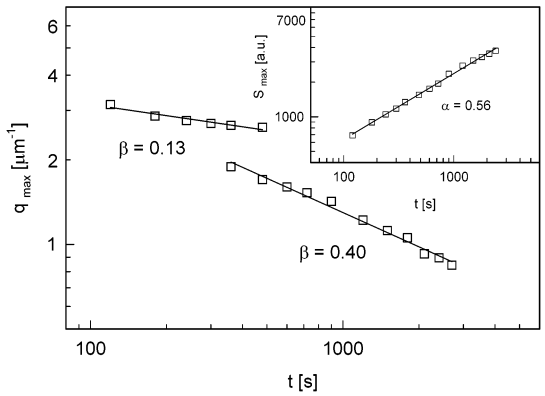


**Figure 17.** Change of the location of the maximum of the scattering intensity $q_{max}$ as a function of time $t$ on a log−log plot, for the I + I region (41 °C) for the thickness of the sample $h = 50\ \mu$m for 90/10% of the 8CB/PS by weight. There is the crossover from the diffusion growth regime with exponent $\beta = 0.13$ to the hydrodynamic growth regime with the exponent $\beta = 0.40$. In the inset − the change of the maximum of the scattering intensity $S_{max}$ as a function of time $t$ on a log−log plot. The growth exponent is $\alpha = 0.56$, indicating that there is no scaling for both regimes.

**Concentration of the Sample 90/10 wt % 8CB/PS.** For the 90/10 wt % mixture on the other hand, the growth processes are very fast in the isotropic phase (45 min), and therefore, we could not determine the exponents in the nematic or smectic matrices. For this composition, we also see two peaks in $S(q,t)$, which grow algebraically in time with different characteristic exponents (Figure 17). For larger wavevectors $\beta = 0.13$, and for smaller $\beta = 0.40$. We also observe that the peak at larger wavevectors merges in a time of 8 min with the peak at smaller wavevectors. We have checked that for such a short time there is no scaling and eq 4 is not obeyed suggesting that there is more than one length scale in the system and that the domains still saturate.

## V. Concluding Remarks

We have proposed a new method of elimination of the multiple scattering of light in the scattering measurements in anisotropic matrices, made during the phase separation of polystyrene (PS) and 8CB liquid crystal in the nematic or smectic phase of 8CB. The multiple scattering effects are due to the different orientations of the LC domains, and they are sufficiently strong to bury the peak coming from the scattering at the interface of PS-rich domains and 8CB-rich domains. In all previous studies, the multiple scattering effects were completely ignored.

Thanks to elimination of the effects of multiple scattering, we could determine the growth laws for polymer domains in the nematic and smectic phase of liquid crystal.

For the phase separation of PS/8CB mixture in the isotropic and smectic phase of 8CB, we have observed two growth regimes: diffusive, characterized by $0.25 < \beta < 0.33$, and the following hydrodynamic growth, characterized by $1 < \beta < {}^3/_2$.

A different exponent $\beta$ in the hydrodynamic regime is caused by the differences in the wetting of properties of phases. Under strong wettability of the glass plates by the isotropic phase of LC, the growth of wetting domains is likely two-dimensional (2d), since the exponent $\beta \approx {}^3/_2$.[16] Under weak wettability of the glass plates by the smectic phase of LC, the wetting domains become

more hemispherical (3d), so we obtain $\beta \approx 1$ (characteristic also for the bulk system[14,16]).

The growth laws do not depend on the film thickness in the isotropic and smectic phase, but they change with the thickness of a film in the nematic phase of a liquid crystal. Here, the exponent $\beta$ increases (from 0.33 to 0.47) with the decreasing of the film thickness (from 120 to 10 $\mu$m).

We suppose, that for small thickness of the samples (10 $\mu$m) the growth of polystyrene domains in the nematic matrix is governed by the elastic forces between the PS domains, arising from the deformations of the director field in orientation of the nematic and leading to $\beta = 0.5$.

We find it surprising that the elastic forces do not seem to affect the growth of PS domains in the smectic matrix. Most probably, the deformation of the smectic matrix lead to the interactions which are repulsive at short distances, thus preventing the domains from coalescence.

In all cases (isotropic, nematic or smectic phase) the scaling rule is obeyed in the first growth regime, governed by diffusion or presumably by elastic forces in the case of thin nematic films.

All these results are obtained for the composition 70/30 wt % of 8CB/PS. The growth laws change with the concentration of the system, probably because of different morphology of studied patterns.

**Acknowledgment.** This work has been supported by the KBN under Grants 2 P03B00923 (2002−2004) and 5 P03B09421.

## References and Notes

(1) Yang, D. K.; Chien, L. C.; Doane, J. W. *Appl. Phys. Lett.* **1992**, *60*, 3102.
(2) Doane, J. W.; Vaz, N. A.; Wu, B.-G.; Zumer, S. *Appl. Phys. Lett.*, **1986**, *48*, 269.
(3) Doane, J. W. *Mater. Res. Soc. Bull.* **1991**, *XVI*, 24.
(4) Kitzerow, H.-S. *Liq. Cryst.* **1994**, *16*, 1.
(5) Kajiyama, T.; Miyamoto, A.; Kikuchi, H.; Morimura, Y. *Chem. Lett.* **1989**, 813.
(6) Doane, J. W. In *Liquid Crystals, Application and Uses*, Bahadur, B., Ed.; World Scientific: Singapore, 1990; Chapter 14.
(7) Wiltzius, P.; Bates, F. S.; Heffner, W. R. *Phys. Rev. Lett.* **1988**, *60*, 1538.
(8) Hashimoto, T. *Phase Transitions* **1988**, *12*, 47.
(9) Langer, J. S. in *Solids far from equilibrium*, Godrèche, C., Ed.; Cambridge University Press: Cambridge, England, 1992.
(10) Gunton, J. D.; San Miguel, M.; Sahni, P. S. In *Phase Transition and Critical Phenomena*; Domb, C., Lebowitz, J. L., Eds.; Academic Press: London, 1983; Vol. 8, pp 267−455.
(11) Bray, A. J. *Adv. Phys.* **1994**, *43*, 357.
(12) Hashimoto, T.; Itakura, M.; Hasegawa, H. *J. Chem. Phys.* **1986**, *85*, 6118.
(13) Furukawa, H. *J. Appl. Crystallogr.* **1988**, *21*, 805.
(14) Siggia, E. D. *Phys. Rev. A* **1979**, *20*, 595.
(15) Shi, B. Q.; Harrison, C.; Cummings, A. *Phys. Rev. Lett.* **1993**, *70*, 206.
(16) Tanaka, H. *Phys. Rev. E.* **1996**, *54*, 1709.
(17) Lapena, A. M.; Glotzer, S. C.; Langer, S. A.; Liu, A. J. *Phys. Rev. E* **1999**, *60*, R29.
(18) Chiu, H.-W.; Kyu, T. *J. Chem. Phys.* **1999**, *110*, 5998.
(19) Zhu, J.; Xu, G.; Ding, J.; Yang, Y. M*acromol. Theory Simul.* **1999**, *8*, 409.
(20) Fiałkowski, M.; Hołyst, R. *Phys. Rev. E* **2002**, *66*, 46121.
(21) Casagrande, C.; Veyssie, M.; Knobler, C. M. *Phys. Rev. Lett.* **1987**, *58*, 2079.
(22) Roux, D.; Knobler, C. M. *Phys. Rev. Lett.* **1988**, *60*, 373.
(23) Kyu, T.; Ilies, I.; Mustafa, M. *J. Phys. IV Colloq. C8* **1993**, *3*, 37.
(24) Poulin, P.; Stark, H.; Lubensky, T. C.; Weitz, D. A. *Science* **1997**, *275*, 1770.
(25) Poulin, P.; Cabuil, V.; Weitz, D. A. *Phys. Rev. Lett.* **1997**, *79*, 4862.
(26) Loudet, J. C.; Poulin, P. *Phys. Rev. Lett.* **2001**, *87*, 165503.
(27) Kuksenok, O. V.; Ruhwandl, R. W.; Shiyanovskii, S. V.; Terentjev, M. *Phys. Rev. E* **1996**, *54*, 5198.
(28) Poulin, P.; Weitz, D. A. *Phys. Rev. E* **1998**, *57*, 626.
(29) Demus, D.; Richter, L. *Textures of Liquid Crystals*, VEB Deutscher Verlag: Leipzig, Germany, 1980.
(30) Ramdane, O. Ou.; Auroy, Ph.; Forget, S.; Raspaud, E.; Martinot-Lagarde Ph.; Dozov, I. *Phys. Rev. Lett.* **2000**, *84*, 3871.
(31) Cluzeau, P.; Poulin, P.; Joly, G.; Nguyen, H. T. *Phys. Rev. E* **2001**, *63*, 031702.
(32) Kao, M. H.; Jester, K. A.; Yodh, A. G. *Phys. Rev. Lett.* **1996**, *77*, 2233.
(33) van Tiggelen, B.; Maynard, R.; Heiderich, A. *Phys. Rev. Lett.* **1996**, *77*, 639.
(34) Stark, H.; Lubensky, T. C. *Phys. Rev. Lett.* **1996**, *77*, 2229.
(35) Wiersma, D. S.; Muzzi, A.; Colocci, M.; Righini, R. *Phys. Rev. Lett.* **1999**, *83*, 4321.
(36) Bohren, C. F.; Huffman, D. R. *Absorption and Scattering of Light by Small Particles*; John Wiley and Sons: New York, 1983; pp 103, 104.
(37) Tanaka, H.; Araki, T. *Europhys. Lett.* **2000**, *51*, 154.

MA034135B